Inorganic Chemistry

Article

pubs.acs.org/IC

Energy Transfer from Sm^{3+} to Eu^{3+} in Red-Emitting Phosphor $LaMgAl_{11}O_{19}:Sm^{3+}$, Eu^{3+} for Solar Cells and Near-Ultraviolet White Light-Emitting Diodes

Xin Min, Zhaohui Huang, Minghao Fang,* Yan-Gai Liu, Chao Tang, and Xiaowen Wu

School of Materials Science and Technology, China University of Geosciences (Beijing), Beijing 100083, P.R. China

ABSTRACT: The red-emitting phosphor $LaMgAl_{11}O_{19}:Sm^{3+}$, Eu^{3+} was prepared by solid-state reaction at 1600 °C for 4 h. The phase formation, luminescence properties, and energy transfer from Sm^{3+} to Eu^{3+} were studied. With the addition of 5 mol % Sm^{3+} as the sensitizer, the excitation wavelength of $LaMgAl_{11}O_{19}:Eu^{3+}$ phosphor was extended from 464 to 403 nm, and the emission intensity under the excitation at 403 nm was also enhanced. The host material $LaMgAl_{11}O_{19}$ could contain the high doping content of Eu^{3+} (20 mol %) without concentration quenching. This energy transfer from Sm^{3+} to Eu^{3+} was confirmed by the decay times of energy donor Sm^{3+}. The mechanism of energy transfer ($Sm^{3+} \rightarrow Eu^{3+}$) was proved to be quadrupole−quadrupole interaction. Under the 403 nm excitation at 150 °C, the emission intensities of the characteristic peaks of Sm^{3+} and Eu^{3+} in $LaMgAl_{11}O_{19}:0.05Sm^{3+}$, $0.2Eu^{3+}$ phosphor were decreased to 65% and 56% of the initial intensities at room temperature, and the relatively high activation energy proved that this phosphor had a good thermal stability. The CIE coordinate was calculated to be (x = 0.601, y = 0.390). The $LaMgAl_{11}O_{19}:0.05Sm^{3+}$, $0.2Eu^{3+}$ phosphor is a candidate for copper phthalocyanine-based solar cells and white light-emitting diodes.

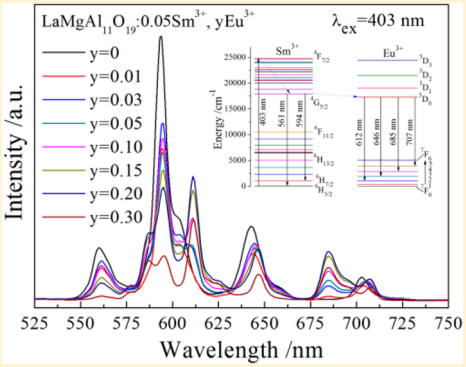

1. INTRODUCTION

Recently, copper phthalocyanine (CuPc), which has a high photovoltaic effect and photoconductivity, has been widely used as an absorber in organic solar cells. However, CuPc-based organic solar cells are still far from practical applications, because of the low efficiency of incident photon energy caused by the limited absorption band in UV and red wavelengths.[1−3] Red-emitting phosphors activated by Eu^{3+} can down-convert the photons in the solar spectrum in the range of 450−470 nm to red photons and increase the efficiency of the incident photon energy for CuPc-based solar cells.[4,5] These red phosphors have also proved to be a good candidate for the application in white light-emitting diodes (w-LEDs).[5−7] However, the excitation wavelength range (450−470 nm) for CuPc still needs to be extended to 400−520 nm, and the Eu^{3+} emission intensity under the excitation at 465 nm for the phosphor-converted w-LEDs also needs to be improved.

Energy transfer from sensitizer to activator could extend the excitation spectrum and enhance the emission of the activator.[8−10] Many sensitizers have been successfully used to expand the Eu^{3+} excitation. Among these sensitizers, the rare-earth ion Sm^{3+} is one of the most effective ions. Sm^{3+} ion can be excited to its $^4F_{7/2}$ energy level at the excitation of 403 nm and then relaxed to the $^4G_{5/2}$ energy level through nonradiative relaxation.[11,12] Like Sm^{3+} ion, the Eu^{3+} ion can be easily relaxed from the high excited state ($^5D_3$) to the $^5D_0$ energy level.[5,13] The energy mismatch between the $^4G_{5/2}$ energy level of Sm^{3+} ion (17 924 cm^{-1}) and the $^5D_0$ energy level of Eu^{3+} ion (17 286 cm^{-1}) is just 638 cm^{-1}, which allows the phonon-assisted energy transfer from the $^4G_{5/2}$ level of Sm^{3+} ion to the $^5D_0$ level of Eu^{3+} ion.[14,15] But the important property, the thermal stability of phosphors in solar cells and w-LEDs, was seldom reported. Moreover, it is very difficult to choose a high-temperature stable material, which can be codoped with the high concentrations of Sm^{3+} and Eu^{3+} ions without concentration quenching.

Lanthanum magnesium hexaluminate ($LaMgAl_{11}O_{19}$), which has a magnetoplumbite-type structure, is characterized by low cost and high physical and chemical stability and can be doped with the high concentration of Eu^{3+} without concentration quenching, compared with other phosphate host matrices.[16−18] Therefore, $LaMgAl_{11}O_{19}$ was selected as a host material for a red-emitting phosphor in CuPc-based solar cells and near-ultraviolet w-LEDs with a blue chip. In this Paper, the $LaMgAl_{11}O_{19}:Sm^{3+}$, Eu^{3+} phosphors were prepared by the high-temperature solid-state method in air atmosphere. The phase structure and luminescent properties were investigated, and investigation results indicated that Sm^{3+} ions could extend the excitation spectrum and enhance emission of Eu^{3+} through energy transfer. Moreover, the energy transfer mechanisms were discussed in detail. The thermal stability of $LaMgAl_{11}O_{19}:Sm^{3+}$, Eu^{3+} phosphor was obtained through the temperature-dependent emission spectra. The CIE chromaticity coordinate was also presented. It is believed that $LaMgAl_{11}O_{19}:0.05Sm^{3+}$, $0.2Eu^{3+}$ phosphor can be used as a red-

Received: February 19, 2014
Published: June 2, 2014

   dx.doi.org/10.1021/ic500412r | Inorg. Chem. 2014, 53, 6060−6065

emitting phosphor for CuPc-based solar cells and white light-emitting diodes.

2. EXPERIMENTAL SECTION

2.1. Materials and Syntheses. The phosphor samples $La_{1-x}MgAl_{11}O_{19}:xSm^{3+}$ (x = 0.005, 0.01, 0.05, 0.1, 0.2), $La_{0.8}MgAl_{11}O_{19}:0.2Eu^{3+}$, and $La_{0.95-y}MgAl_{11}O_{19}:0.05Sm^{3+}$, yEu^{3+} (y = 0.01, 0.03, 0.05, 0.1, 0.15, 0.2, 0.3) were synthesized by the high-temperature solid-state reaction method. $Al(OH)_3$ (99.9%), $Mg(OH)_2$ (99.9%), La_2O_3 (99.9%), Sm_2O_3 (99.9%), and Eu_2O_3 (99.9%) were used as raw materials. La_2O_3 powders, which could absorb atmospheric water rapidly, were weighed immediately after heating at 1100 °C for 1 h. These raw materials were well-mixed in an agate mortar according to their stoichiometric amounts. The homogeneous mixtures were molded by uniaxial pressing at 15 MPa and then put into a crucible with a lid. The crucible was calcined at 1600 °C for 4 h and cooled to room temperature naturally. The sintered samples were ground into powders for measurement.

2.2. Characterization Method. The crystalline phases of the phosphors were analyzed by using X-ray diffraction (XRD, D8 Advance diffractometer, Bruker Corporation, Germany) with Cu Kα (λ = 1.5406 Å) radiation. The room-temperature photoluminescence excitation (PLE) and emission (PL) spectra were recorded by a fluorescence spectrophotometer (F-4600, Hitachi, Japan) with a photomultiplier tube operating at 500 V. A 150 W Xe lamp was used as the excitation source. The room-temperature decay curves were characterized on a spectrofluorometer (Horiba, Jobin Yvon TBX-PS), and a 460 nm pulse laser radiation was used as the excitation source. The temperature-dependent emission spectra were measured on the spectrophotometer (F-4600, Hitachi, Japan), which was combined with a self-made heating attachment and a computer-controlled electric furnace. The quantum yield was recorded by a fluoromax-4 spectrofluorometer (Horiba, Jobin Yvon) with an integral sphere at room temperature.

3. RESULTS AND DISCUSSION

3.1. Phase Analysis. Figure 1 shows the XRD patterns of phosphors $LaMgAl_{11}O_{19}:Sm^{3+}$, $LaMgAl_{11}O_{19}:Eu^{3+}$, and $LaMgAl_{11}O_{19}:Sm^{3+}$, Eu^{3+}. The JCPDS card (No. 78−1845) of $LaMgAl_{11}O_{19}$ is also presented for a comparison. From Figure 1, it can be seen that all the XRD patterns are well-matched with the $LaMgAl_{11}O_{19}$ phase without any other impurity phase. At the same time, the radii of Sm^{3+} ion (0.96 Å) and Eu^{3+} ion (0.95 Å) are very close to that of La^{3+} ion (1.06 Å). Therefore, we can conclude that Sm^{3+} and Eu^{3+} ions can be doped easily to replace the La^{3+} ions in the $LaMgAl_{11}O_{19}$ lattice without any structural changes.

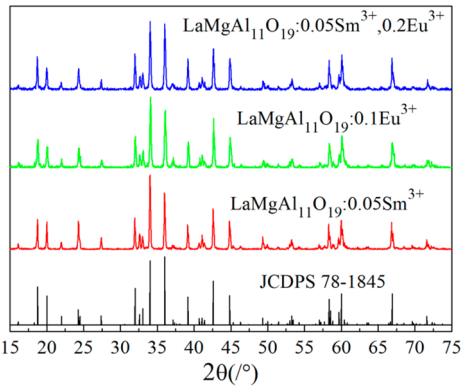

Figure 1. X-ray diffraction patterns of $LaMgAl_{11}O_{19}:Sm^{3+}$, $LaMgAl_{11}O_{19}:Eu^{3+}$, $LaMgAl_{11}O_{19}:Sm^{3+}$, Eu^{3+}, and the JCPDS card (No. 78−1845) of $LaMgAl_{11}O_{19}$.

3.2. Luminescence Properties of $LaMgAl_{11}O_{19}:Sm^{3+}$, Eu^{3+}. The PL and PLE spectra of the Sm^{3+}- and Eu^{3+}-doped $LaMgAl_{11}O_{19}$ phosphors are shown in Figure 2a,c, respectively. As shown in Figure 2a, the strongest excitation peak among the PLE spectrum is the peak at 403 nm, corresponding to the $^6H_{5/2}\rightarrow {}^4F_{7/2}$ transition monitored at 594 nm.[11,19] The $LaMgAl_{11}O_{19}:Sm^{3+}$ phosphors exhibited an orange-reddish emission band at 561, 594, 644, and 704 nm under the excitation at 403 nm because of the $^4G_{5/2}\rightarrow {}^6H_{J/2}$ (J = 5, 7, 9, and 11) transitions of Sm^{3+}.[11,19] The emission intensity increases quickly with the increase in the Sm^{3+} concentration, reaches its maximum value when the concentration is 5 mol %, and then decreases because of the concentration quenching effect (Figure 2b). Therefore, the optimum Sm^{3+} doping concentration for $LaMgAl_{11}O_{19}$ is 0.05 mol. Figure 2c shows the red emission of $LaMgAl_{11}O_{19}:Eu^{3+}$ under the excitation at 464 nm, due to $^5D_0\rightarrow {}^7F_K$ (K = 1, 2, 3, 4, and 5) transitions, respectively.[15,20] The PLE spectrum of $LaMgAl_{11}O_{19}:Eu^{3+}$ phosphor monitored at 612 nm consists of three excitation peaks. The main broad excitation band (200−390 nm) with a maximum value at 305 nm corresponds to a strong charge transition broad band absorption CTS ($O^{2-}\rightarrow Eu^{3+}$), and the other two excitation peaks at 396 and 464 nm are mainly caused by the strong f→ f transition absorption of Eu^{3+} ($^7F_0\rightarrow {}^5L_6$ and $^7F0\rightarrow {}^5D_2$).[15,20] However, the emission spectra of $LaMgAl_{11}O_{19}:Sm^{3+}$ and $LaMgAl_{11}O_{19}:Eu^{3+}$ phosphors, under excitation at 464 and 403 nm, are both very weak. Therefore, it is possible to enhance the PL and expand the PLE spectra of Eu^{3+} ion. The PL and PLE spectra of Sm^{3+}- and Eu^{3+}-*co*-doped $LaMgAl_{11}O_{19}$ phosphor are presented in Figure 3. The PLE spectrum of the $LaMgAl_{11}O_{19}:Sm^{3+}$, Eu^{3+} phosphor monitored at 594 nm is similar to that at 612 nm, while the relative intensities of the peaks are different. In the PL spectrum shown in Figure 3a, six significant emission peaks at 561, 594, 612, 646, 685, and 707 nm are observed, and these peaks correspond to the $^4G_{5/2}\rightarrow {}^6H_{5/2}$ and $^4G_{5/2}\rightarrow {}^6H_{7/2}$ transitions of Sm^{3+} and the $^5D_0\rightarrow {}^7F_2$, $^5D_0\rightarrow {}^7F_3$, $^5D_0\rightarrow {}^7F_4$, $^5D_0\rightarrow {}^7F_5$ transitions of Eu^{3+}, respectively. The emission band in the range from 575 to 625 nm can also be decomposed into five well-decomposed Gaussian components centered at 587, 596, and 612 nm for Eu^{3+} ions and 594 and 605 nm for Sm^{3+} ions (Figure 3b).

The PL spectra of $LaMgAl_{11}O_{19}:0.05Sm^{3+}$, yEu^{3+} (y = 0, 0.01, 0.03, 0.05, 0.1, 0.15, 0.2, 0.3) samples under the excitation at 403 nm are presented in Figure 4. The PL spectra with different Eu^{3+} concentrations contain the characteristic peaks of Sm^{3+} and Eu^{3+}, as mentioned above. It also can be seen that only strong emission peaks of Sm^{3+} are recorded when Eu^{3+} is not doped. Moreover, the Sm^{3+} emission intensity is significantly decreased with the increase of the added Eu^{3+} ions due to the energy transfer from Sm^{3+}. However, the characteristic emission intensity of Eu^{3+} increases when the doping concentration of Eu^{3+} is increased from 0.01 to 0.2 mol and then decreases because of concentration quenching. These results further indicate energy transfer from Sm^{3+} to Eu^{3+} with the high doping concentration.

To analyze the mechanism of energy transfer from Sm^{3+} to Eu^{3+}, the luminescent decay curves of the $^4G_{5/2}\rightarrow {}^6H_{7/2}$ transition of Sm^{3+} were measured in the $LaMgAl_{11}O_{19}:0.05Sm^{3+}$ and $LaMgAl_{11}O_{19}:0.05Sm^{3+}$, yEu^{3+} (y = 0.01, 0.03, 0.1, 0.2, 0.3) phosphors, as shown in Figure 5a. It can be seen that the decay curve decays rapidly with the increase of Eu^{3+} content. In addition, lifetimes and energy transfer (ET) efficiencies are calculated (Figure 5b). According to the results

dx.doi.org/10.1021/ic500412r | Inorg. Chem. 2014, 53, 6060−6065

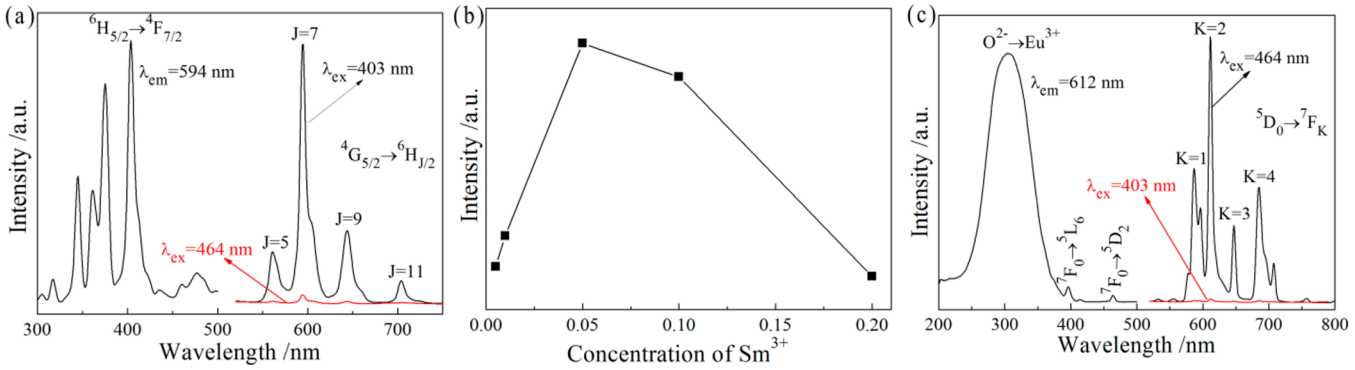

Figure 2. (a) PLE and PL spectra of $LaMgAl_{11}O_{19}$:xSm^{3+}; (b) PL intensity of phosphors vs the Sm^{3+} concentration; (c) PLE and PL spectra of $LaMgAl_{11}O_{19}$:$0.2Eu^{3+}$.

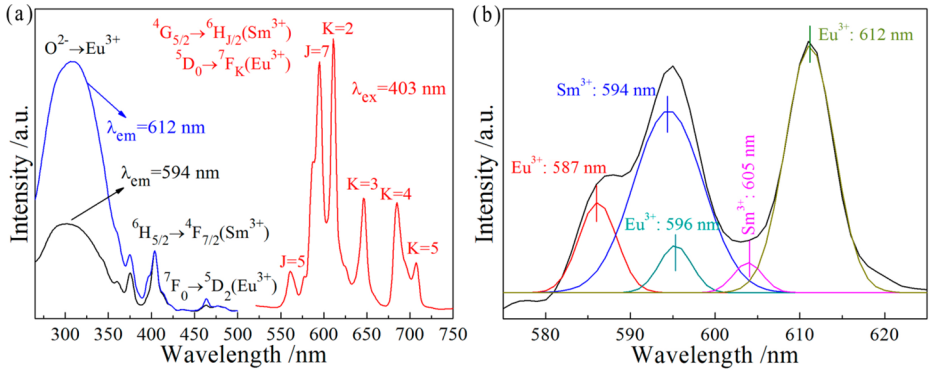

Figure 3. (a) PLE (left) and PL (right) spectra of $LaMgAl_{11}O_{19}$:$0.05Sm^{3+}$, $0.2Eu^{3+}$ phosphor; (b) the deconvolution of the PL spectra by Gaussian fitting between 575 and 625 nm.

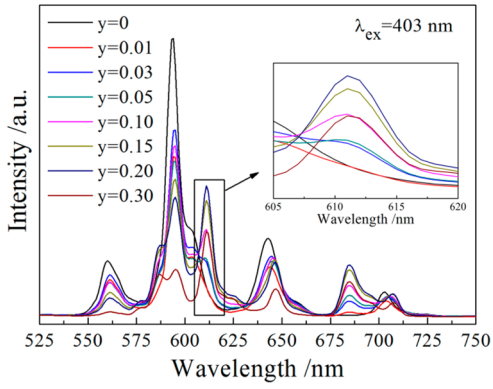

Figure 4. PL spectra of $LaMgAl_{11}O_{19}$:$0.05Sm^{3+}$, yEu^{3+} phosphor with different Eu^{3+} concentrations under the excitation at 403 nm.

by Blasse and Grabmaier,[21] the decay behavior can be expressed as

$$I = I_0 \exp(-t/\tau) \quad (1)$$

where I and I_0 are the luminescence intensity at the time t and initial time, respectively; τ is the lifetime. According to eq 1 and the decay curves shown in Figure 5a, the lifetimes of the 594 nm emission of Sm^{3+} were calculated to be 1.62, 1.58, 1.53, 1.40, 1.22, and 0.91 ms, which are decreased with the increase of the Eu^{3+} concentration in $LaMgAl_{11}O_{19}$:$0.05Sm^{3+}$, yEu^{3+} (y = 0.01, 0.03, 0.1, 0.2, 0.3). The energy transfer efficiency is calculated by

$$\eta_T = 1 - \tau_s/\tau_{s0} \quad (2)$$

where η_T is the energy transfer efficiency, and τ_s and τ_{s0} are the lifetimes of the sensitizer (Sm^{3+}) with and without the activator (Eu^{3+}). As shown in Figure 5b, the energy transfer efficiency increases with the increase of the Eu^{3+} content. The energy transfer efficiency of $LaMgAl_{11}O_{19}$:$0.05Sm^{3+}$, $0.2Eu^{3+}$ is calculated to be 24.8%. All these results strongly prove the energy transfer from Sm^{3+} to Eu^{3+}.[22,23]

There are two major energy transfer mechanisms: exchange interaction and multipolar interaction. The prerequisite of exchange interaction mechanism is that the sensitizer should be close to the activator.[24] Therefore, we mainly discuss the multipolar interaction for energy transfer from Sm^{3+} to Eu^{3+} in $LaMgAl_{11}O_{19}$. As described by Dexter's energy transfer expressions of multipolar interaction and Reisfeld's approximation,[25] the ratio of the luminescence quantum efficiency of the sensitizer with activation to the efficiency of the sensitizer without activation can be defined as

$$I_{S0}/I_S \propto C^{n/3} \quad (3)$$

where I_{S0} and I_S are the luminescence intensities of the $LaMgAl_{11}O_{19}$:Sm^{3+} with the absence and presence of Eu^{3+} ion obtained after Gaussian fitting as illustrated above; C is the sum of the concentration of Sm^{3+} and Eu^{3+}; n = 6, 8, 10 represent dipole−dipole (d−d), dipole−quadrupole (d−q), and quadrupole−quadrupole (q−q) interactions, respectively.[25,26] Figure 6a−c shows the linear relationship between I_{S0}/I_S and $C^{n/3}$, and the values of R^2 with n = 6, 8, and 10 are also presented. The best linear relationship is obtained when n = 10, indicating that the mechanism of energy transfer from Sm^{3+} to Eu^{3+} is a q−q interaction.

dx.doi.org/10.1021/ic500412r | Inorg. Chem. 2014, 53, 6060−6065

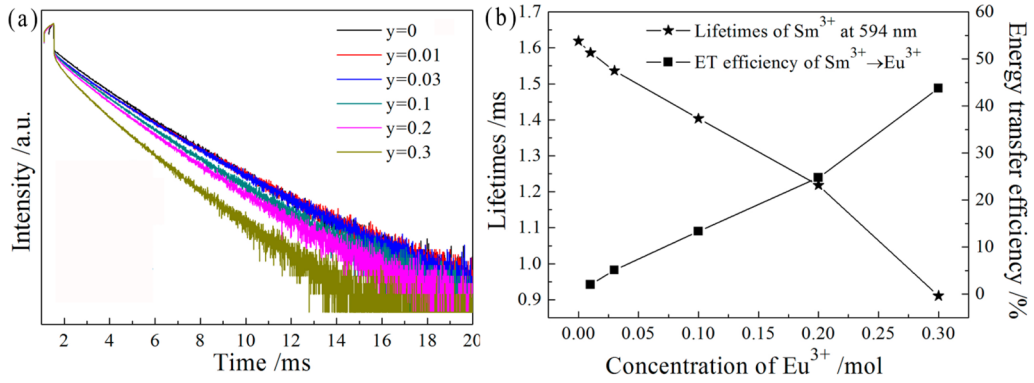

Figure 5. (a) The photoluminescence decay curves of Sm^{3+} in $LaMgAl_{11}O_{19}$:0.05Sm^{3+}, 0.2Eu^{3+} phosphor (excited at 460 nm and monitored at 594 nm). (b) The dependence of the lifetimes and energy transfer efficiency on Eu^{3+} doping concentration.

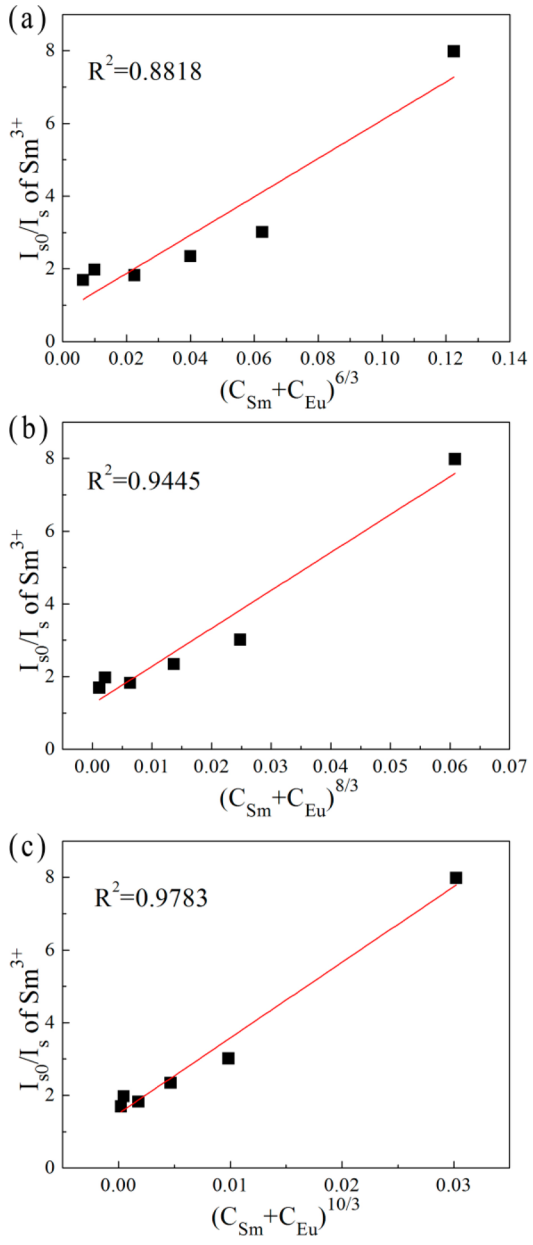

Figure 6. Dependence of I_{S0}/I_S of Sm^{3+} on (a) $(C_{Sm} + C_{Eu})^{6/3}$, (b) $(C_{Sm} + C_{Eu})^{8/3}$, and (c) $(C_{Sm} + C_{Eu})^{10/3}$.

The energy transfer process was further studied and presented in an energy level diagram (Figure 7). Sm^{3+} ion is

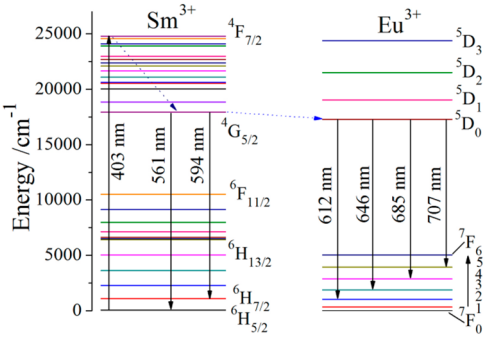

Figure 7. Schematic diagram of energy levels of Sm^{3+} and Eu^{3+} in the $LaMgAl_{11}O_{19}$:Sm^{3+}, Eu^{3+} phosphors.

excited to the $^4F_{7/2}$ level by 403 nm light, and then relaxed to the $^4G_{5/2}$ level by nonradiative relaxation. The energy of the $^4G_{5/2}$ level for Sm^{3+} relax to the $^6H_{7/2}$ and $^6H_{5/2}$ levels and present the emission peaks at 561 and 594 nm, respectively. At the same time, the energy of Sm^{3+} is also transferred to the $^5D_0$ level of Eu^{3+} by the resonance between the two levels,[8] and the emission intensity of Sm^{3+} partly decreases. Therefore, the characteristic emission peaks at 612, 646, 685, and 707 nm are observed and enhanced due to the $^5D_0 \rightarrow {}^7F_K$ (K = 2, 3, 4, and 5) transitions of Eu^{3+} ion. For the $^4G_{5/2}$ energy level of Sm^{3+} ion is 638 cm^{-1} higher than the $^5D_0$ energy level of Eu^{3+} ion, the energy transfer from Eu^{3+} to Sm^{3+} would hardly happen.

3.3. Thermal Stability, CIE, and Quantum Yield of $LaMgAl_{11}O_{19}$:0.05Sm^{3+}, 0.2Eu^{3+}. In the application of CuPc-based solar cells and high-power w-LEDs, the thermal stability for phosphors is an important factor to consider. The emission spectra of $LaMgAl_{11}O_{19}$:0.05Sm^{3+}, 0.2Eu^{3+} sample under the excitation at 403 nm and different temperatures are shown in Figure 8. The intensity of the emission spectrum decreases with the increase of the temperature. The inset shows the comparison results of the thermal luminescence quenching of $LaMgAl_{11}O_{19}$:0.05Sm^{3+}, 0.2Eu^{3+} at the characteristic emission of Sm^{3+} and Eu^{3+} obtained after Gaussian fitting. When the temperature rises to 150 °C, the emission intensities of the characteristic peaks of Sm^{3+} and Eu^{3+} are decreased to 58% and 53% of the initial intensities at room temperature, respectively.

dx.doi.org/10.1021/ic500412r | Inorg. Chem. 2014, 53, 6060−6065

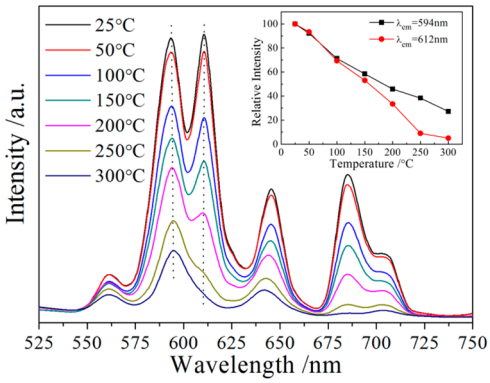

Figure 8. PL spectra (λ_{ex} = 403 nm) of $LaMgAl_{11}O_{19}$:0.05Sm^{3+}, 0.2Eu^{3+} phosphor at different temperatures (25−300 °C). The inset shows the comparison results of PL intensities of $LaMgAl_{11}O_{19}$:0.05Sm^{3+}, 0.2Eu^{3+} at the characteristic emission of Sm^{3+} and Eu^{3+} as a function of the temperature.

To understand the temperature dependence, the activation energy for the characteristic emission of Sm^{3+} and Eu^{3+} was calculated by the Arrhenius equation[27]

$$I_T = I_0/[1 + C\exp(-\Delta E/kT)] \quad (4)$$

where I_0 and I_T is the emission intensity of the phosphor obtained after Gaussian fitting at room temperature and other different temperatures; ΔE is the activation energy for thermal quenching; C is a constant; and k is the Boltzmann constant (8.62×10^{-5} eV). The plot of $\ln[(I_0/I_T) - 1]$ versus $1/kT$ and the activation energy of the characteristic emission of Sm^{3+} and Eu^{3+} are shown in Figure 9. The activation energy values at 594 and 612 nm are calculated to be 0.24 and 0.3 eV, which indicate that the phosphor with a good thermal stability can be used in CuPc-based solar cells and high-power w-LEDs.

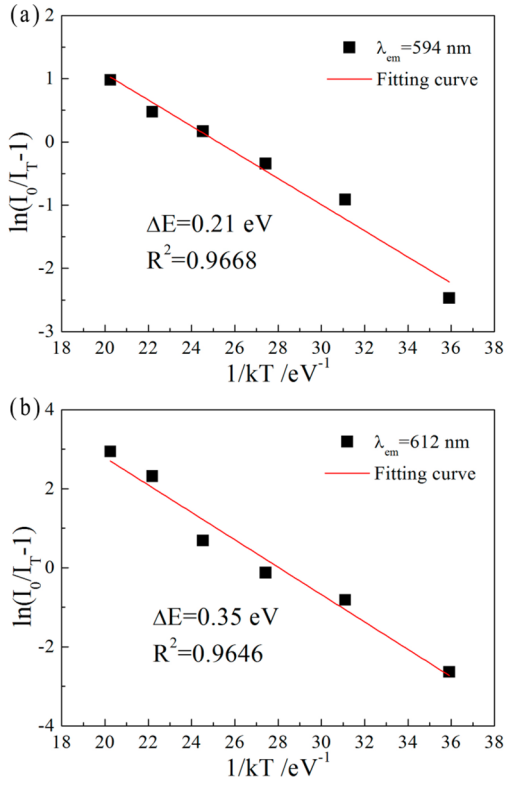

Figure 9. Plot of $\ln[(I_T/I_0) - 1]$ vs $1/kT$ activation energy for thermal quenching of the characteristic emission of Sm^{3+} (a) and Eu^{3+} (b) in $LaMgAl_{11}O_{19}$:0.05Sm^{3+}, 0.2Eu^{3+} phosphors.

The CIE chromaticity coordinates for the $LaMgAl_{11}O_{19}$:0.05Sm^{3+}, 0.2Eu^{3+} sample under the excitation at 403 nm is calculated to be (x = 0.601, y = 0.390), which indicates this phosphor is applicable for commercial applications according to the coordinates of the commercially available red-emitting phosphor Y_2O_2S:Eu^{3+} (x = 0.668, y = 0.332).[8]

The quantum yield is also an important parameter for the practical application of phosphors. We measured the quantum yields of $LaMgAl_{11}O_{19}$:0.05Sm^{3+}, $y$$Eu^{3+}$ and $LaMgAl_{11}O_{19}$:0.1Eu^{3+} phosphors. Under the excitation at 403 nm, the recorded quantum yields of $LaMgAl_{11}O_{19}$:0.05Sm^{3+} y = 0, 0.01, 0.03, 0.05, 0.1, 0.15, 0.2, and 0.3 are 0.34, 0.25, 0.3, 0.29, 0.3, 0.41, 0.48, and 0.14, respectively. The quantum yield is 0.33 for $LaMgAl_{11}O_{19}$:0.1Eu^{3+} phosphor under the excitation at 464 nm.

4. CONCLUSIONS

In this Paper, the red-emitting phosphors $LaMgAl_{11}O_{19}$: Sm^{3+}, Eu^{3+} were synthesized by the high-temperature solid-state reaction method. The emission intensity of $LaMgAl_{11}O_{19}$:Sm^{3+}, Eu^{3+} phosphors under near-ultraviolet excitation at 403 nm was enhanced successfully due to the high doping content of Eu^{3+} (20 mol %) without concentration quenching. The excitation spectrum of $LaMgAl_{11}O_{19}$:Sm^{3+}, Eu^{3+} phosphors was also extended from 464 to 405 nm because of the energy transfer from Sm^{3+} to Eu^{3+}. The analyses of PL and decay curves confirmed the energy transfer from Sm^{3+} to Eu^{3+}. The energy transfer efficiency and lifetime of $LaMgAl_{11}O_{19}$:0.05Sm^{3+}, 0.2Eu^{3+} sample were calculated to be 24.8% and 1.22 ms, respectively. In addition, the mechanism of energy transfer was the q−q interaction, according to the study results based on Dexter's formula and Reisfeld's approximation. The temperature-independent PL properties also proved that this phosphor had a good thermal stability. The CIE coordinate of $LaMgAl_{11}O_{19}$:0.05Sm^{3+}, 0.2Eu^{3+} was calculated to be (x = 0.601, y = 0.390). All these indicated that $LaMgAl_{11}O_{19}$:0.05Sm^{3+}, 0.2Eu^{3+} phosphor could be applied in CuPc-based solar cells and w-LEDs.

AUTHOR INFORMATION

Corresponding Author

*E-mail: fmh@cugb.edu.cn.

Notes

The authors declare no competing financial interest.

ACKNOWLEDGMENTS

This work was financially supported by the National Natural Science Foundation of China (NSFC Grant No. 51172216) and the Fundamental Research Funds for the Central Universities (Grant No. 2652013051).

REFERENCES

(1) Singh, V. P.; Parsarathy, B.; Singh, R. S.; Aguilera, A.; Anthony, J.; Payne, M. *Sol. Energy Mater. Sol. Cells* **2006**, *90*, 798−812.
(2) Yakimov, A.; Forrest, S. R. *Appl. Phys. Lett.* **2002**, *80*, 1667−1669.
(3) Tsutsui, T.; Nakashima, T.; Fujita, Y.; Saito, S. *Synth. Met.* **1995**, *71*, 2281−2282.
(4) Lin, H. Y.; Fang, Y. C. *J. Am. Ceram. Soc.* **2010**, *93*, 3850−3856.
(5) Lin, H. Y.; Fang, Y. C.; Huang, X. R.; Chu, S. Y. *J. Am. Ceram. Soc.* **2010**, *93*, 138−141.

(6) Neeraj, S.; Kijima, N.; Cheetham, A. K. *Chem. Phys. Lett.* **2004**, *387*, 2−6.
(7) Wang, Z.; Liang, H.; Zhou, L.; Wu, H.; Gong, M.; Su, Q. *Chem. Phys. Lett.* **2005**, *412*, 313−316.
(8) Won, Y. H.; Jang, H. S.; Im, W. B.; Jeon, D. Y. *J. Electrochem. Soc.* **2008**, *155*, J226−J229.
(9) Lee, G. H.; Kim, T. H.; Yoon, C.; Kang, S. *J. Lumin.* **2008**, *128*, 1922−1996.
(10) Biju, P. R.; Jose, G.; Thomas, V.; Nampoori, V. P. N.; Unnikrishnan, N. V. *Opt. Mater.* **2004**, *24*, 671−677.
(11) Tiana, Y.; Liu, Y.; Hua, R. N.; Na, L. Y.; Chen, B. J. *Mater. Res. Bull.* **2012**, *47*, 59−62.
(12) Kumar, V.; Bedyal, A. K.; Pitale, S. S.; Ntwaeaborwa, O. M.; Swart, H. C. *J. Alloys Compd.* **2013**, *554*, 214−220.
(13) Ozawa, L.; Jaffe, P. M. *J. Electrochem. Soc.* **1971**, *118*, 1678−1679.
(14) Carnall, W. T.; Fields, P. R.; Rajnak, K. *J. Chem. Phys.* **1968**, *49*, 4424−4442.
(15) Carnall, W. T.; Fields, P. R.; Rajnak, K. *J. Chem. Phys.* **1968**, *49*, 4450−4455.
(16) Min, X.; Fang, M. H.; Huang, Z. H.; Liu, Y. G.; Jiang, B.; Hu, M. L. *Rare Met. Mater. Eng.* **2013**, *42*, 646−649.
(17) Min, X.; Fang, M. H.; Huang, Z. H.; Liu, Y. G.; Tang, C.; Qian, T. T.; Wu, X. W. *Ceram. Int.* **2014**, *40*, 4535−4539.
(18) Singh, V.; Watanabe, S.; Gundu Rao, T. K.; Kwak, H. Y. *Solid State Sci.* **2010**, *12*, 1981−1987.
(19) Lin, H.; Yang, D.; Liu, G.; Ma, T.; Zhai, B.; An, Q.; Yu, J.; Wang, X.; Liu, X.; Pun, E. Y. B. *J. Lumin.* **2005**, *113*, 121−128.
(20) Wang, Z. J.; Li, P. L.; Yang, Z. P.; Guo, Q. L. *J. Optoelectron., Laser* **2011**, *22*, 718−721.
(21) Blasse, G.; Grabmaier, B. C. *Luminescent Materials;* Springer-Verlag: Berlin, Germany, 1994.
(22) Shionoya, S.; Yen, W. M. *Phosphor Handbook;* CRC Press: Boca Raton, FL, 1998.
(23) Zhu, H. K.; Xia, Z. G.; Liu, H. K.; Mi, R. Y.; Hui, Z. *Mater. Res. Bull.* **2013**, *48*, 3513−3517.
(24) Garcia Sole, J.; Bausa, L. E.; Jaque, D. *An Introduction to the Optical Spectroscopy of Inorganic Solids;* John Wiley & Sons, Ltd.: West Sussex, England, 2005.
(25) Dexter, D. L.; Schulman, J. H. *J. Chem. Phys.* **1954**, *22*, 1063−1071.
(26) Yang, W. J.; Luo, L.; Chen, T. M.; Wang, N. S. *Chem. Mater.* **2005**, *17*, 3883−3888.
(27) Zhang, S. Y.; Huang, Y. L.; Nakai, Y.; Tsuboi, T.; Seo, H. J. *J. Am. Ceram. Soc.* **2011**, *94*, 2987−2992.